

Exercise session Numerical Linear Algebra: matrix compression in practice

1 Linear-time ACA

You have previously seen *Adaptive Cross Approximation* (ACA) as an effective compression scheme. In this section we will devise a linear-time version. **Recall the theoretical form of ACA from the lecture notes, and show its equivalence to the form given in algorithm 1.** What is the complexity of algorithm 1? Be precise.

Algorithm 1: Linear-time ACA	
	input : Block $B(\mathbf{t}, \mathbf{s}) \in \mathbb{C}^{\mathbf{t} \times \mathbf{s}}$, tolerance tol output: Low-rank approx $B(\mathbf{t}, \mathbf{s}) \approx B_r = XY^T$, $X \in \mathbb{C}^{\mathbf{t} \times r}$, $Y \in \mathbb{C}^{\mathbf{s} \times r}$
1	init $\epsilon := 1$, $k = 0$
2	while $\epsilon > \text{tol}$ do
3	select pivot $(i_k, j_k) \in \mathbf{t} \times \mathbf{s}$;
4	$\mathbf{x}_k := B(:, j_k)$, $\mathbf{y}_k := B(i_k, :)$;
5	$\mathbf{x}_k := \mathbf{x}_k - \sum_{\mu < k} \mathbf{x}_\mu \mathbf{y}_\mu(j_k)$;
6	$\mathbf{y}_k := \mathbf{y}_k - \sum_{\mu < k} \mathbf{x}_\mu(i_k) \mathbf{y}_\mu$;
7	set $\mathbf{x}_k := \frac{1}{\mathbf{x}_k(i_k)} \mathbf{x}_k$ or $\mathbf{y}_k := \frac{1}{\mathbf{y}_k(j_k)} \mathbf{y}_k$;
8	$X = [X, \mathbf{x}_k]$, $Y = [Y, \mathbf{y}_k]$;
9	$\epsilon := \ \mathbf{x}_k\ \ \mathbf{y}_k\ / (\ \mathbf{x}_0\ \ \mathbf{y}_0\)$;
10	$k := k + 1$
11	end

Implement algorithm 1 on the matrices provided in `matrices.zip`. Compare the obtained rank to the numerical rank obtained using

the SVD. What do you observe? Can you explain this?

2 ACA-CUR

You have seen that, at least theoretically, if the ACA algorithm selects pivots $\{i_1, \dots, i_k\}$ and $\{j_1, \dots, j_k\}$, then

$$B(\mathbf{t}, \mathbf{s}) \approx B_r = XY^T = B(:, \mathbf{s})B(\mathbf{t}, \mathbf{s})^{-1}B(\mathbf{t}, :).$$

Verify this claim numerically. Use for the inverse both the matlab function ‘inv’ and ‘\’. What do you observe? Explain.

We will outline here a way we can stably, on the fly, factorize $B(\mathbf{t}, \mathbf{s})^{-1}$. To do so, we look first at theorem 1

Theorem 1. *Suppose algorithm 1 is used to factor the block $B(\mathbf{t}, \mathbf{s})$, and the pivots selected during its run are $(\mathbf{t}_r, \mathbf{s}_r) = ([i_1, \dots, i_r], [j_1, \dots, j_r])$. We adopt the convention that in line 7 \mathbf{x}_k is set to \mathbf{x}_k/d_k or \mathbf{y}_k is set to \mathbf{y}_k/d_k , and let $\mathbf{t}_k, \mathbf{s}_k$ correspondingly denote the index sets selected up to step k of the algorithm. Then*

$$B_r = X_r Y_r^T = B(:, \mathbf{s}_r) U_{\mathbf{s}_r} D_r U_{\mathbf{t}_r}^T B(\mathbf{t}_r, :) \quad (1)$$

with $D_r := \text{diag}(d_1, \dots, d_r)^{-1}$ and $U_{\mathbf{t}_r}, U_{\mathbf{s}_r} \in \mathbb{C}^{r \times r}$ upper triangular matrices defined by

$$U_{j_1} = 1, \quad U_{i_1} = 1$$

and

$$U_{\mathbf{s}_{k+1}} = \begin{bmatrix} U_{\mathbf{s}_k} & -U_{\mathbf{s}_k} D_k U_{\mathbf{t}_k}^T B(\mathbf{t}_k, :) \mathbf{e}_{j_{k+1}} \\ \mathbf{0}^T & 1 \end{bmatrix} \quad (2)$$

and similarly for $U_{\mathbf{t}_{k+1}}$.

You have been provided a ‘naive’ implementation of this idea. **Compare this to algorithm 2. What is different?**

Implement algorithm 2. Compare the numerical accuracy of the naive implementation to the accuracy of algorithm 2, over decreasing user-supplied tolerance. What do you observe?

Algorithm 2: ACA-CUR

input : Matrix $B(\mathbf{t}, \mathbf{s}) \in \mathbb{C}^{\mathbf{t} \times \mathbf{s}}$, tolerance **tol**
output: Low-rank CUR approx. $B(\mathbf{t}, \mathbf{s}) \approx B(:, \mathbf{s}_r)U_{\mathbf{s}_r}D_rU_{\mathbf{t}_r}^TB(\mathbf{t}_r, :)$
1 **init** $\epsilon := \infty$, $k = 0$, $\mathbf{t}_0 = \mathbf{s}_0 = \emptyset$, $U_{\mathbf{t}_0} = U_{\mathbf{s}_0} = D_0 = []$
2 **while** $\epsilon > \mathbf{tol}$ **do**
3 select pivot $(i_k, j_k) \in \mathbf{t} \times \mathbf{s}$;
4 $d_k = B(i_k, j_k) - (B(i_k, \mathbf{s}_k)U_{\mathbf{s}_k})D_k(U_{\mathbf{t}_k}^TB(\mathbf{t}_k, j_k))$;
5 $\mathbf{b}_k = D_k \cdot (U_{\mathbf{t}_k}^TB(\mathbf{t}_k, j_k))$;
6 $\mathbf{a}_k^T = D_k \cdot (B(i_k, \mathbf{s}_k)U_{\mathbf{s}_k})$;
7 $U_{\mathbf{s}_{k+1}} = \begin{bmatrix} U_{\mathbf{s}_k} & -U_{\mathbf{s}_k}\mathbf{b}_k \\ \mathbf{0}^T & 1 \end{bmatrix}$;
8 $U_{\mathbf{t}_{k+1}} = \begin{bmatrix} U_{\mathbf{t}_k} & -U_{\mathbf{t}_k}^T\mathbf{a}_k \\ \mathbf{0}^T & 1 \end{bmatrix}$;
9 $D_{k+1} = \begin{bmatrix} D_k & \\ & 1/d_k \end{bmatrix}$;
10 $\mathbf{t}_{k+1} = \mathbf{t}_k \cup i_k$, $\mathbf{s}_{k+1} = \mathbf{s}_k \cup j_k$;
11 $\mathbf{x}_k = B(:, \mathbf{s}_k)U_{\mathbf{s}_k}$, $\mathbf{y}_k^T = U_{\mathbf{t}_k}^TB(\mathbf{t}_k, :)$;
12 $\epsilon := \|\mathbf{x}_k\| \|\mathbf{y}_k\| / (\|\mathbf{x}_0\| \|\mathbf{y}_0\|)$;
13 $k := k + 1$;
14 **end**

3 Hierarchical matrices for the Helmholtz equation

The Helmholtz equation is an important equation in mathematics and physics. It models monochromatic wave scattering, both acoustic and electro-magnetic. We consider in this section the Helmholtz equation in an open domain $\Omega \subseteq \mathbb{R}^3$ with (weakly) Lipschitz boundary $\partial\Omega = \partial\Omega_D \cup \partial\Omega_N$, on which respectively Dirichlet and Neumann boundary conditions are imposed:

$$\begin{cases} \nabla^2 u + \kappa^2 u &= 0, & \text{in } \Omega \\ u &= g_D, & \text{on } \partial\Omega_D \\ \frac{\partial u}{\partial \mathbf{n}} &= g_N, & \text{on } \partial\Omega_N \end{cases} \quad (3)$$

and we require u to satisfy the *Sommerfeld radiation condition*, i.e.

$$\lim_{\mathbf{r} \rightarrow \infty} \mathbf{r} \cdot \left(\frac{\partial u}{\partial \mathbf{r}} - \imath \kappa u \right) = 0. \quad (4)$$

Using the method of Green's functions it can be shown that, for $\mathbf{x} \in \Omega$

$$u(\mathbf{x}) = - \underbrace{\int_{\partial\Omega_D} [\gamma_1 u] G(\mathbf{x}, \mathbf{y}) d\mathbf{y}}_{:=\text{SLP}([\gamma_1 u])(\mathbf{x})} + \underbrace{\int_{\partial\Omega_N} [\gamma_0 u] \frac{\partial}{\partial \mathbf{n}_y} G(\mathbf{x}, \mathbf{y}) d\mathbf{y}}_{:=\text{DLP}([\gamma_0 u])(\mathbf{x})} \quad (5)$$

in which γ_0, γ_1 denote the trace and conormal derivative respectively, $[\cdot]$ denotes the jump across the boundary, and

$$G(\mathbf{x}, \mathbf{y}) := \frac{\exp(\imath \kappa \|\mathbf{x} - \mathbf{y}\|)}{4\pi \|\mathbf{x} - \mathbf{y}\|}$$

is the *Green's kernel* for the 3D Helmholtz equation. Setting $[\gamma_1 u] = \varphi$ and $[\gamma_0 u] = \psi$, and taking the trace and conormal derivative of equation (5) we obtain, on $\partial\Omega$:

$$\begin{aligned} g_D(\mathbf{x}) &= - \underbrace{\int_{\partial\Omega_D} G(\mathbf{x}, \mathbf{y}) \varphi(\mathbf{y}) d\mathbf{y}}_{(\mathcal{S}\varphi)(\mathbf{x})} \pm \frac{1}{2} \psi(\mathbf{x}) + \underbrace{\int_{\partial\Omega_N} \frac{\partial}{\partial \mathbf{n}_y} G(\mathbf{x}, \mathbf{y}) \psi(\mathbf{y}) d\mathbf{y}}_{(\mathcal{D}\psi)(\mathbf{x})} \\ g_N(\mathbf{x}) &= \pm \frac{1}{2} \varphi(\mathbf{x}) - \underbrace{\int_{\partial\Omega_D} \frac{\partial}{\partial \mathbf{n}_x} G(\mathbf{x}, \mathbf{y}) \varphi(\mathbf{y}) d\mathbf{y}}_{(\mathcal{D}'\varphi)(\mathbf{x})} + \gamma_1 \underbrace{\int_{\partial\Omega_N} \frac{\partial}{\partial \mathbf{n}_y} G(\mathbf{x}, \mathbf{y}) \psi(\mathbf{y}) d\mathbf{y}}_{-(\mathcal{W}\psi)(\mathbf{x})} \end{aligned}$$

in which the 4 main boundary integral operators (BIOS) for the Helmholtz equation have been introduced: $\mathcal{S}, \mathcal{D}, \mathcal{D}', \mathcal{W}$, respectively the single-layer, double-layer, adjoint double-layer and hypersingular boundary operators. **You do not need to understand this fully, this is just some background for the curious.**

In particular, sound-soft scattering is modelled by setting

$$\mathcal{S}u_{sc} = -u_{in}$$

where u_{sc} is the scattered field and u_{in} is the incoming acoustic pressure field, typically a plane wave.

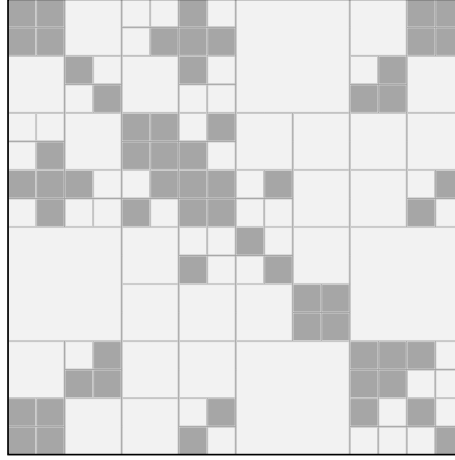


Figure 1: Illustration of the block structure of an \mathcal{H} -matrix. dark gray blocks correspond to non-admissible cluster-cluster interactions.

The integral kernel G is separable at long distances, meaning that upon Galerkin discretization of the operator \mathcal{S} , the blocks corresponding to well-separated clusters are low-rank. This gives rise to a so-called *Hierarchical Matrix* (\mathcal{H} -matrix). Large, off-diagonal blocks are low rank, while the diagonal blocks, and small off-diagonal blocks are dense, as in figure 1. Often, the low-rank blocks are compressed using ACA. **You have been provided code that computes an \mathcal{H} -matrix approximation to S . Look at the code provided. Re-write your ACA scheme to be of the form**

```
[A,B,flag]=aca(row,col,n,m,tol)
```

Where ‘flag’ is a boolean that is 1 if the low-rank compression failed, and ‘row’ and ‘col’ are functions that, given i or j , return the i th row or the j th column, as (column) vectors. Run the \mathcal{H} -matrix compression scheme for some wavenumbers varying from $.1\kappa_{\max}$ to $.9\kappa_{\max}$. Look at the console output and compute the data sparsity for the far-field. What do you observe?